Computational Analysis of Pulsed Radiofrequency Ablation in Treating Chronic Pain

Sundeep Singh[1] and Roderick Melnik[1,2(✉)]

[1] MS2Discovery Interdisciplinary Research Institute, Wilfrid Laurier University, 75 University Avenue West, Waterloo, ON N2L 3C5, Canada
rmelnik@wlu.ca

[2] BCAM - Basque Center for Applied Mathematics, Alameda de Mazarredo 14, 48009 Bilbao, Spain

Abstract. In this paper, a parametric study has been conducted to evaluate the effects of frequency and duration of the short burst pulses during pulsed radiofrequency ablation (RFA) in treating chronic pain. Affecting the brain and nervous system, this disease remains one of the major challenges in neuroscience and clinical practice. A two-dimensional axisymmetric RFA model has been developed in which a single needle radiofrequency electrode has been inserted. A finite-element-based coupled thermo-electric analysis has been carried out utilizing the simplified Maxwell's equations and the Pennes bioheat transfer equation to compute the electric field and temperature distributions within the computational domain. Comparative studies have been carried out between the continuous and pulsed RFA to highlight the significance of pulsed RFA in chronic pain treatment. The frequencies and durations of short burst RF pulses have been varied from 1 Hz to 10 Hz and from 10 ms to 50 ms, respectively. Such values are most commonly applied in clinical practices for mitigation of chronic pain. By reporting such critical input characteristics as temperature distributions for different frequencies and durations of the RF pulses, this computational study aims at providing the first-hand accurate quantitative information to the clinicians on possible consequences in those cases where these characteristics are varied during the pulsed RFA procedure. The results demonstrate that the efficacy of pulsed RFA is significantly dependent on the duration and frequency of the RF pulses.

Keywords: Chronic pain · Pulsed radiofrequency ablation · Brain and nervous system · Finite element analysis · Pennes bioheat transfer

1 Introduction

Radiofrequency ablation (RFA) of painful nerves has been gaining increasing popularity among pain management therapists for reducing certain kinds of chronic pain, which represent complex diseases ultimately involving the brain and nervous system. Among them are low back pain, hip pain, knee pain and migraine, to name just a few [1–4]. The complexity of linkages that produces pathophysiology in these diseases

J. M. F. Rodrigues et al. (Eds.): ICCS 2019, LNCS 11539, pp. 436–450, 2019.
https://doi.org/10.1007/978-3-030-22747-0_33

would ideally require multiscale modelling [5]. RFA is a minimally invasive treatment modality whereby electromagnetic energy in the frequency range of 300–500 kHz is applied to make discrete therapeutic lesions. The lesion formed interrupts the conduction of nociceptive signals and blocks the pain transmission from reaching the central nervous system. Apart from RFA, several other non-surgical ablative modalities have been used for the treatment of painful nerves, viz., cryoablation and chemical neurolysis [6]. However, RFA stands out to be the most effective and widely applied modality for alleviating chronic pain, as compared to its counterparts. Importantly, RFA is not a curative procedure and does not treat the root cause of pain, but it anesthetizes the source of patient's pain that usually lasts for about 12 months [7].

The RFA system for nerve ablation usually comprises of three main components: (a) radiofrequency (RF) generator for generation of high frequency ($\sim$500,000 Hz) alternating currents, (b) a fully insulated 20–22 gauge electrode needle with 5–10 mm exposed tip, and (c) dispersive ground plate having large surface area. During the RFA procedure, a high-frequency alternating current is delivered from the generator to the RF electrode and flows from the uninsulated electrode tip through the biological tissue to the dispersive ground electrode. The interaction of high-frequency alternating current with the biological tissue initiates the rapid oscillations of charged molecules (mainly proteins) that generates heat. The rate of this ionic heating will be higher around the uninsulated active tip of the electrode, where the current density is largest [7, 8]. The lethal temperature during the application of RFA for treating target nerve in mitigating chronic pain is considered to be at or above 45–50 °C. Moreover, it is highly undesirable, if the temperature within the biological tissue goes beyond 100 °C during the RFA procedure, as it would result in tissue boiling, vaporization and charring. Indeed, it is known that the charring results in an abrupt rise in the electrical impedance of the tissue surrounding the active tip of the electrode, limiting any further conduction of the thermal energy and acting as a barrier, restricting the energy deposition and reducing the size of ablation volume [9, 10].

The power delivery during the RFA application can be done using either continuous or pulsed modes. In the conventional continuous power delivery mode, a high-frequency alternating current is delivered from the RF generator to the electrode placed close to the target nerve to heat the neural tissue (80–90 °C). This causes protein denaturation and destruction of the axons and stops the transmission of nociceptive signals from the periphery [8]. However, in the pulsed RFA, brief 'pulses' of RF signals are applied from the RF generator to the neural tissue followed by silent phases that allow time for heat dissemination. Also, the pulsed RFA can produce far stronger electrical fields as compared to the continuous RFA. Initially, the pulsed RFA was thought to be a completely non-destructive procedure for mitigating chronic pain, but recent research in the field suggests that there are both thermal and non-thermal effects of the pulsed RFA procedure [7]. What currently known is that, during the pulsed RFA, clinical effects are not only caused by the high-frequency alternating electrical current leading to heat-generated lesion, but also by the intense electric fields causing a change in the cellular behavior [11]. Importantly, the pulsed RFA procedure is less destructive as compared to the conventional continuous RFA, as there have been no reports of neurological side effects [7].

Several feasibility studies have been reported utilizing the application of the pulsed RFA in treating some of chronic pain conditions [12–18]. Although several available clinical studies on pulsed RFA techniques portray their effectiveness, especially among patients who suffer from radicular pain and peripheral neuropathies, the exact explanation of the mechanisms of action during the pulsed RFA still remains elusive [7]. Thus, further research is needed to determine the clinical effectiveness of pulsed RFA among different chronic conditions for long term pain relief. In view of the above, the present computational study aims to evaluate the efficacy of the pulsed RFA, focusing on the key input characteristics such as frequencies and durations of the RF pulses. While at the final stage, the efficacy of any therapeutic modality needs to be evaluated and justified by clinical studies, the systematic computational analysis could play a crucial role by serving as a quick, convenient and inexpensive tool for studying the thermo-electric performance of the treatment modality under the influence of varying input parameters.

The challenges associated with modelling the heterogeneous surrounding associated with the target nerve that includes, bones, muscle and other critical structures have precluded the development of comprehensive mathematical models in this field, where the brain and nervous system becomes an important part for consideration in multiscale approaches [5]. Moreover, accurately addressing the significant variations among the thermo-electric properties of these tissues in the numerical model of RFA could become problematic, especially, if the non-linear variations of these properties are to be considered in the coupled analysis. Furthermore, the modelling of the pulsed RFA procedure could become even more challenging in those cases where we need to capture accurately the impact of small pulses of millisecond durations, rapidly altering in between lower and maximum applied energy levels, on the temperature distribution during the numerical analysis. In addressing some of the above challenges, we have developed a model to analyze the pulsed RFA procedure for treating chronic pain within the biological tissues and evaluated the impact of durations and frequencies of RF pulses delivered by the commercially available RF generators on the efficacy of the pulsed RFA procedure.

2 Materials and Methods

This section provides details of the computational geometry, mathematical and computational models, along with main materials parameters and thermo-electric characteristics.

2.1 Description of the Computational Model

Figure 1 shows the two-dimensional axisymmetric computational domain considered in the present study that comprises of the muscle tissue with a single needle RF electrode. The dimensions of this domain have been chosen consistently with those available in the literature (e.g., [19]). The pulsed RFA has been performed utilizing a 22-gauge needle electrode with the active tip length of 10 mm. The considered

thermo-electric properties in the present study at the frequency range of 500 kHz are given in Table 1 [11, 19, 20].

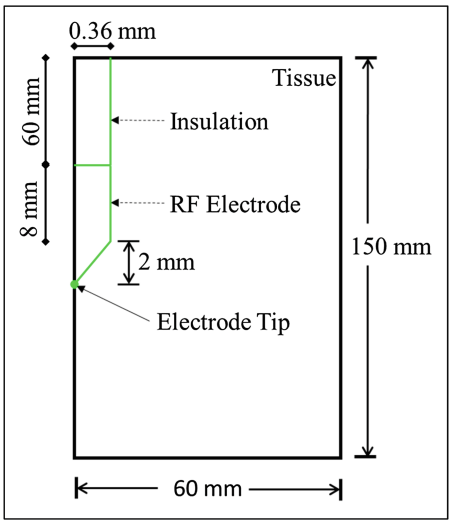

Fig. 1. Two-dimensional axisymmetric pulsed RFA model considered in the present study.

Table 1. Thermo-electric properties of different materials applied in this study [11, 19, 20].

Material (Tissue/Electrode)	Electrical conductivity σ (S/m)	Specific heat capacity c (J/kg/K)	Thermal conductivity k (W/m/K)	Density ρ (kg/m^3)
Tissue	0.446	3421	0.49	1090
Insulation	10^{-5}	1045	0.026	70
Electrode	7.4×10^6	480	15	8000

2.2 Governing Equations

The pulsed RFA procedure represents a coupled thermo-electric problem whereby electromagnetic energy is applied to heat the biological tissue. Importantly, the electric field distribution within the computational domain has been computed by using the simplified version of the Maxwell's equations, known as quasi-static approximation. The governing equation for the electrical problem is represented by

$$\nabla \cdot (\sigma \nabla V) = 0, \tag{1}$$

where σ is the electrical conductivity (S/m) and V is the electric potential (V). The volumetric heat generated Q_p (W/m^3) due to the ionic agitation [10] within the

biological tissue caused by the high-frequency alternating current during the pulsed RFA procedure [11] is evaluated by

$$Q_p = \mathrm{J} \cdot \mathrm{E}, \tag{2}$$

where the electric field intensity E (V/m) and current density J (A/m^2) can be derived from the following Eqs. 3 and 4, respectively

$$\mathrm{E} = -\nabla V, \tag{3}$$

$$\mathrm{J} = \sigma\, \mathrm{E} \tag{4}$$

Due to the complicity in microscale anatomical structures of biological tissues, a detailed microscopic study of the heat transfer within such tissues is a very challenging task. In the context of RFA procedures, it is usually sufficient to have the information on the heat transport within biological tissues at a phenomenological scale much larger than the microscale of cells and voids, while, much smaller than the system length scale [21]. The present study, also, considers a macroscale approach for modelling the heat transfer phenomenon within the biological tissue during the RFA procedures, whereby the biological tissue has been considered as a mixture of the two continuum deformable media, blood and tissues. We have applied a scaling of the global balance equations to derive our equations at the macroscopic scale [21]. Furthermore, the temperature distribution during the pulsed RFA procedure has been obtained using the Fourier-law-based Pennes bioheat transfer equation

$$\rho c \frac{\partial T}{\partial t} = \nabla \cdot (k \nabla T) - \rho_b c_b \omega_b (T - T_b) + Q_m + Q_p \tag{5}$$

Where ρ (kg/m^3) is the density, c (J/kg/K) is the specific heat capacity, k (W/m/K) is the thermal conductivity, ρ_b is the density of blood (1050 kg/m^3), c_b is the specific heat capacity of blood (3617 J/kg/K), ω_b is the blood perfusion rate within the tissue (6.35×10^{-4} s^{-1}), Q_p (W/m^3) is the ionic heat generated during RFA and is computed using Eq. 2 above, Q_m (W/m^3) is the metabolic heat generation that has been neglected due to its insignificant contribution during RFA [19], T_b is the blood temperature (37 °C), T is the unknown tissue temperature to be computed from Eq. 5 and t (s) is the duration of the pulsed RFA procedure.

The novelty of the present consideration is in the evaluation of the impact of the commercially available RF generators pulse durations (10 to 50 ms) and pulse frequencies (1 to 10 Hz) on the efficacy of the pulsed RFA procedure. The present study highlights the significance of the pulsing algorithm in comparison to the continuous RF power supply. The temperature distribution within the biological tissue along with the charring temperatures at the tip of the RF electrode for different cases considered in the present study have been reported to provide a critical information about such input characteristics to the clinicians during the pulsed RFA procedure.

2.3 Initial and Boundary Conditions

The initial temperature in the model has been set to 37 °C, which resembles the internal temperature of the human body. The initial voltage, before the onset of the pulsed RFA procedure, has been considered to be zero. A pulsed voltage (with the maximum applied voltage of 45 V) has been applied at the active uninsulated portion of the RF electrode, while 0 V electric potential has been applied on the outer boundaries of the computational domain, simulating the ground pads. Further, electrical and thermal continuity boundary conditions have been imposed at each interface of our computational domain. The ablation volume has been quantified by the isotherm temperature of 50 °C (i.e. the volume within the computational domain having temperature ≥ 50 °C at the end of the pulsed RFA procedure). Figure 2 represents the schematic of the pulse train applied at the active tip of the electrode during the pulsed RFA procedure. Importantly, the train of RF burst pulses applied during the pulsed RFA procedure, as reported in previous clinician studies, varies from 10 to 20 ms in duration and from 1 to 10 Hz in repetition frequency [11, 22]. In view of the above, the present numerical study evaluates the effects of variation in the duration and frequencies of RF pulses during the pulsed RFA procedure. In what follows, we analyze two main situations: (a) the different values of the duration of RF pulses are set to 10 ms, 20 ms, 30 ms, 40 ms and 50 ms, respectively, at the pulse frequency of 2 Hz; (b) the different values of the frequency of RF pulses are set to 1 Hz, 2 Hz, 6 Hz and 10 Hz, respectively, with the pulse duration of 20 ms. Such a consideration has been motivated by [23].

2.4 Numerical Setup and Computational Details

The computational model of the pulsed RFA procedure (shown in Fig. 1) has been solved numerically after imposing the necessary initial and boundary conditions mentioned earlier. The spatial and temporal temperature distributions during the RFA procedures have been obtained by solving the Pennes bioheat transfer equation (Eq. 5). A finite-element method (FEM) based commercial COMSOL Multiphysics [24] software has been utilized to solve the coupled thermo-electric problem of the pulsed RFA procedure. The computational domain has been discretized using a heterogeneous triangular mesh elements using COMSOL's built-in mesh generator with a finer mesh size at the electrode-tissue interface, where the highest thermal and electrical gradients are expected. A convergence analysis has been carried out in order to determine the optimum mesh element size that will lead to mesh-independent solution and reduce the computational cost. The electric field of the coupled thermo-electric problem has been found by using "multifrontal massively parallel sparse direct solver" (MUMPS) with default pre-ordering algorithm. The iterative conjugate gradient method with geometric multi-grid pre-smoothers has been used to determine the temperature field. The relative tolerance has been set to 10^{-5} and the numerical convergence has been attained below this pre-specified value for all simulations. The implicit time-stepping method backward differentiation formulas (BDF) has been used to solve the time-dependent problem and care has been taken to store the data at each steps by assigning strict steps

to the solvers. The convergence of the coupled thermo-electric FEM problem is further improved by using segregated algorithms that splits the solution process into sub-steps. Importantly, the coupling is achieved by iterating the entire process after the application of segregated algorithms to resolving physical fields in a sequential manner (e.g., thermal and electrical). The great advantage of chosen approach is that an optimal iterative solver can be used in each sub-step, thus solving a smaller problem in a computationally efficient way. Although this approach generally does require more iterations until convergence, each iteration takes significantly less time compared to one iteration of the fully coupled approach, thus reducing the total solution time and memory usage. All simulations have been conducted on a Dell T7400 workstation with Quad-core 2.0 GHz Intel® Xeon® processors. The mean computation time for each simulation was 3 h.

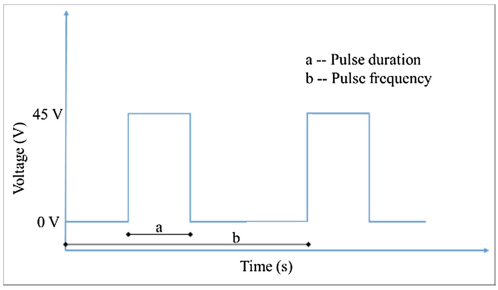

Fig. 2. Schematic view of the pulse train applied to the pulsed RFA model in this study.

3 Results and Discussion

Our main focus is on the effects of the duration and the frequency of the RF pulses and the influence of these effects on the efficacy of the pulsed RFA procedure. As mentioned earlier, a parametric study has been conducted with the applied voltage of 45 V for two different scenarios, (a) with a fixed pulse frequency of 2 Hz and different durations, viz., 10 ms, 20 ms, 30 ms, 40 ms and 50 ms, respectively, and (b) with a fixed pulse duration of 20 ms and different frequencies, viz., 1 Hz, 2 Hz, 6 Hz and 10 Hz, respectively. Importantly, the combination of 2 Hz frequency and 20 ms RF pulse duration is widely used in clinical practices with the applied voltage of 45 V during the pulsed RFA procedure [14, 19]. In what follows, we will explore different aspects of altering the critical input parameters, viz., duration and frequency of the RF pulses, during the pulsed RFA procedure and compare the results with the standard protocol (45 V–20 ms–2 Hz).

Firstly, a comparison study has been conducted between the continuous RFA and pulsed RFA (20 ms–2 Hz) to evaluate the temperature distribution with the applied voltage of 45 V. Figure 3 depicts the temperature distribution as a function of time at

the tip of the RF electrode within few seconds after the initiation of RFA application for these two cases. To our surprise, with the applied voltage of 45 V the charring temperature of 100 °C has been reached at the active tip of the RF electrode within less than 1 s during continuous RFA, as shown in Fig. 3(a). The temperature distribution within the first 2.5 s of pulsed RFA (45 V–20 ms–2 Hz) procedure has been depicted in Fig. 3(b). As evident from Fig. 3(b), the pulsed RFA protocol results in the formation of alternating temperature spikes that are located between the lower and higher values pertaining to the duration and frequency of the applied pulse train, restricting or delaying the occurrence of charring. As mentioned earlier, the charring is highly undesirable phenomena during the RFA procedure that results in dramatic increase of the impedance and prevents the RF power generator from delivering further energy within the biological tissue [9, 25, 26]. Different strategies are developed and adopted in clinical practices to either mitigate or delay the occurrence of charring during the RFA procedure by either modifying the RF delivery protocol or the RF electrode [10]. However, during the pulsed RFA procedure (45 V–20 ms–2 Hz), some dissipation of even such high energy is allowed within the biological tissue without the occurrence of charring. This is due to the fact that during the pulsed RFA procedure, periods of high-energy deposition (45 V) are rapidly alternating with the periods of low-energy deposition (0 V). It allows tissue cooling adjacent to the RF electrode during the periods of minimal energy deposition and subsequently leads to a greater energy deposition which, in its turn, results in deeper heat penetration and greater tissue coagulation. The differences between the temperature distributions within the biological tissue obtained after 1 s of continuous and pulsed RFA procedures have been presented in Fig. 4. Further, Fig. 5 depicts the propagation of damage volume corresponding to the 50 °C isotherm at different time steps using the standard pulsed RFA procedure.

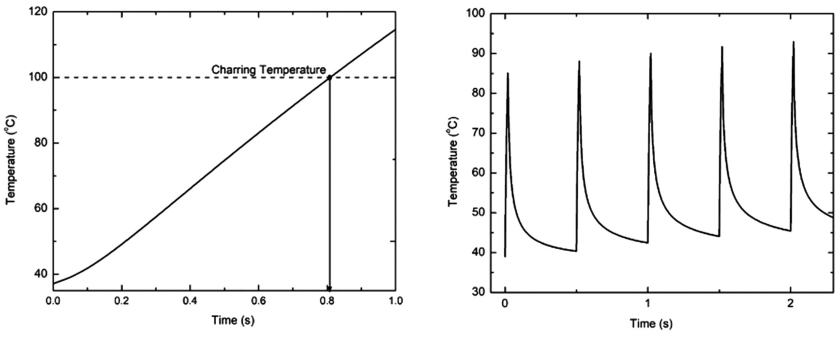

Fig. 3. Temperature distribution monitored at the tip of the RF electrode for: (a) continuous RFA and (b) pulsed RFA procedures.

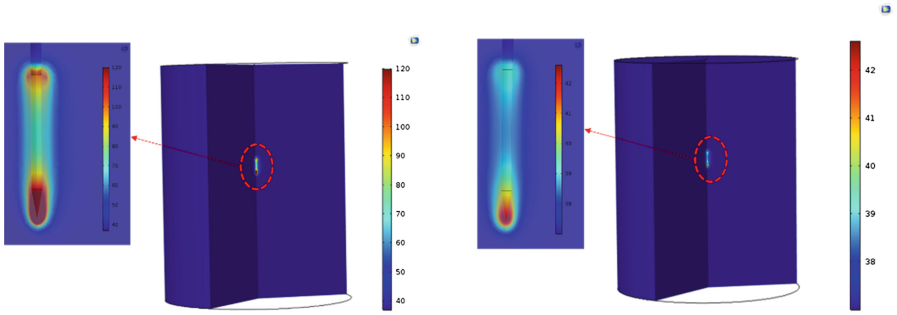

Fig. 4. (Color online) Temperature distribution within the biological tissue after 1 s of the RFA procedure: (a) for the continuous mode and (b) for the pulsed mode.

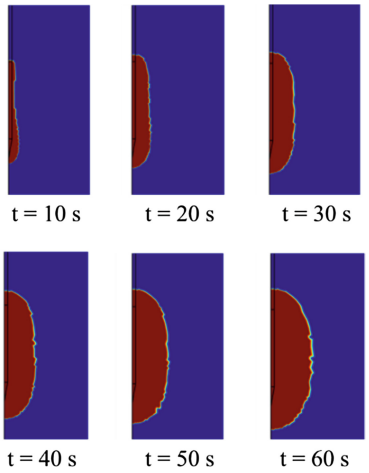

Fig. 5. (Color online). Propagation of damage volume at different time steps during the pulsed RFA procedure.

Figure 6 presents the temperature distribution obtained after 60 s of standard pulsed RFA (45 V–20 ms–2 Hz) procedure as a function of distance measured along a line perpendicular to the electrode tip. As evident from Fig. 6, the charring has not occurred even after 90 s of pulsed RFA application, even in the case when the voltage of 45 V has been applied. At the same time, the charring has been noticed within less than 1 s of continuous RFA application. Thus, the pulsed RFA protocol results in efficient dissipation of the applied RF energy as compared to the continuous RF protocols, thereby enabling the generation of a large size ablation volume.

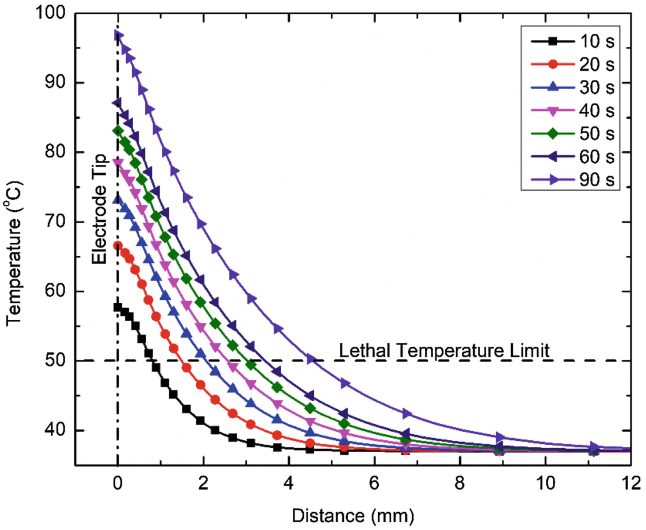

Fig. 6. (Color online). Temperature distribution as a function of distance monitored along the line perpendicular to the tip of the RF electrode during the standard pulsed RFA procedure.

The effects of different RF pulse durations (viz., 10 ms, 20 ms, 30 ms, 40 ms and 50 ms) on the average value of temperature monitored at the active tip of RF electrode as a function of time during the pulsed RFA procedure for treating chronic pain has been presented in Fig. 7. As evident from Fig. 7, there prevails a significant variation in the temperature profile among different cases considered in the present study. The target tip temperature increases with increasing the RF pulse duration and vice-versa. Furthermore, the increase in RF pulse duration beyond 20 ms makes it more susceptive to the occurence of charring within the biological tissue. Figure 8 presents the temperature distribution obtained after 60 s of the pulsed RFA procedure, along the line perpendicular to the tip of the RF electrode for fixed pulse frequency of 2 Hz, but different values of the pulse durations, viz., 10 ms, 20 ms, 30 ms, 40 ms and 50 ms, respectively. It can be seen from Fig. 8 that up to 20 ms durations of RF pulses no charring has occured after 60 s of the pulsed RFA procedure. Figure 9 depicts the temperature distribution after 60 s of the pulsed RFA procedure with different durations of the RF pulses considered in this study. As evident from Fig. 9, a small region of tissue has been charred with the RF pulse duration of 30 ms, and the charring region significantly increases for the duration of 40 ms and 50 ms, respectively.

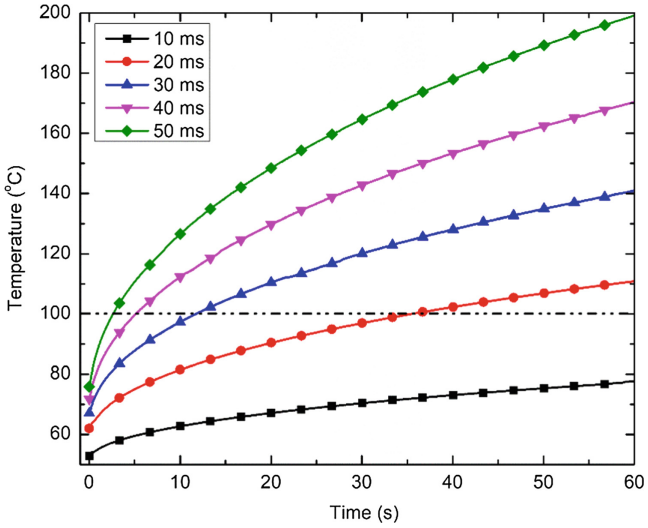

Fig. 7. (Color online). Average value of temperature profile as a function of time monitored at the active tip of the RF electrode for pulse frequency of 2 Hz and different values of pulse durations considered in the present study.

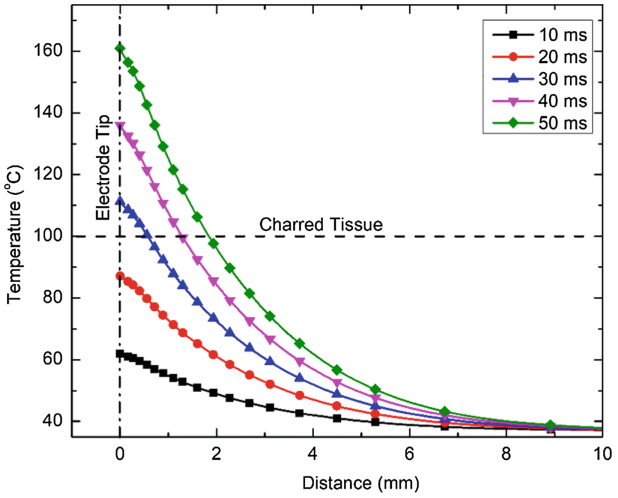

Fig. 8. (Color online). Temperature distribution as a function of distance monitored along the line perpendicular to the tip of the RF electrode for different values of RF pulse durations.

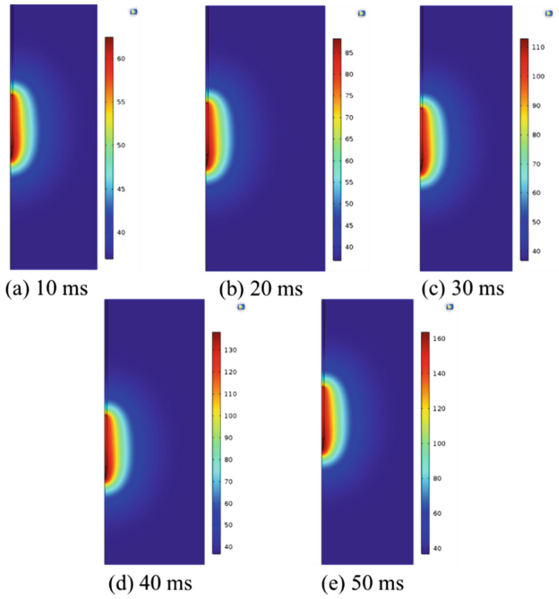

Fig. 9. (Color online). Temperature distribution obtained after 60 s of pulsed RFA application for different values of RF pulse durations considered in the present study.

Figure 10 presents the effects of different RF pulse frequencies (viz., 1 Hz, 2 Hz, 6 Hz and 10 Hz) with a fixed pulse duration of 20 ms on the average value of temperature monitored at the active tip of RF electrode as a function of time. It can be seen from Fig. 10 that significant variations prevail in the temperature profile among different cases considered in this study. Particularly, the average value of target tip temperature reaches the charring temperature within less than 5 s for the RF pulse frequencies of 6 Hz and 10 Hz, respectively. These results demonstrate the importance of variations in the RF pulses, their durations and frequencies, on the temperature distribution obtained at active tip of the electrode and within the biological tissue. Indeed, such variations can lead to significant quantitative and qualitative changes in the scenarios of the attainment of charring within the biological tissue. Thus, *a priori* reasonable choice of these parameters need to be made during the treatment planning stage of the therapeutic procedure, so as to minimise the risk and perform safe and reliable procedure. The reported results would provide the clinicians with deeper insight in the selection of pulses durations and frequencies during the pulsed RFA procedures for chronic pain relief. Importantly, the synergy between the durations and frequencies RF pulses would result in greater absorption of the RF energy and thereby increasing the ablation volume during the pulsed RFA procedure for treating chronic pain.

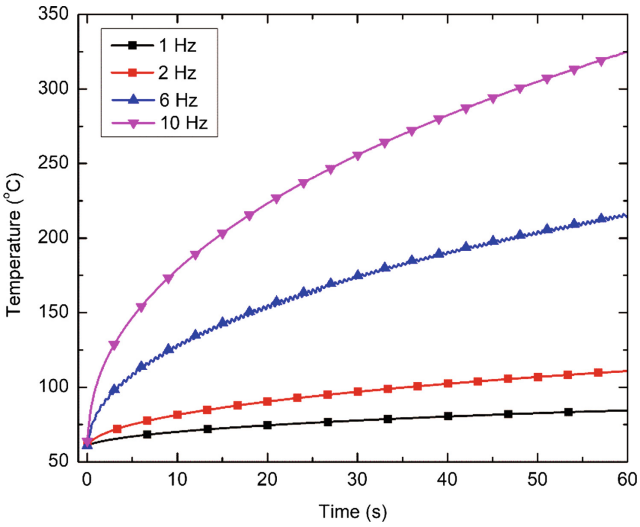

Fig. 10. (Color online). Average value of temperature profile as a function of time monitored at the active tip of the RF electrode for pulse duration of 20 ms and different values of pulse frequencies considered in the present study.

The next step in this study would be to consider a fully heterogeneous surrounding, including the target nerve and the bone, in the three-dimensional model along with the temperature-dependent thermo-electric properties and the temperature-controlled algorithms. We also plan to include the actual models of nerve damage (i.e. mitigation of pain signals). This would enhance the capability of our model even further, since the current model uses a simplified approach of defining the lesion/ablation zone with temperature isotherms during the modelling of the pulsed RFA procedure for treating chronic pain. While our current results provide the critical information on the variation of RF pulses, their durations and frequencies, the development of the model mentioned above will likely provide even better correlation with the clinical scenarios.

4 Conclusion

In this work, a comparative computational study has been conducted to evaluate the temperature distribution between the continuous and pulsed RFA procedures. The effect of durations and frequencies of short burst RF pulses on the efficacy of the pulsed RFA procedure for mitigating chronic pain has been systematically evaluated. Major challenges in developing comprehensive multiscale mathematical models in this field have been highlighted. The reported results revealed that the pulsed RFA could result in greater dissipation of the RF energy as compared to the continuous RFA. This likely occurs due to certain delay in the manifestation of charring owing to the alternating cooling cycles of the RF pulses. Further, it has been found that the increase in both duration and frequency of the RF pulses during pulsed RFA procedures could result in

an increase of temperature distribution within the biological tissue and vice-versa. However, the consideration of optimized combination of duration and frequency of RF pulses would considerably reduce the chances of charring and/or would lead to a better RF energy distribution within the tissue along with generation of a large ablation volume during such procedures.

Acknowledgements. Authors are grateful to the NSERC and the CRC Program for their support. RM is also acknowledging support of the BERC 2018-2021 program and Spanish Ministry of Science, Innovation and Universities through the Agencia Estatal de Investigacion (AEI) BCAM Severo Ochoa excellence accreditation SEV-2017-0718.

References

1. Leggett, L.E., Soril, L.J., Lorenzetti, D.L., et al.: Radiofrequency ablation for chronic low back pain: a systematic review of randomized controlled trials. Pain Res. Manag. **19**(5), 146–154 (2014)
2. Bhatia, A., Yasmine, H., Philip, P., Steven, P.C.: Radiofrequency procedures to relieve chronic hip pain: an evidence-based narrative review. Reg. Anesth. Pain Med. **43**(1), 72–83 (2018)
3. Bhatia, A., Philip, P., Steven, P.C.: Radiofrequency procedures to relieve chronic knee pain: an evidence-based narrative review. Reg. Anesth. Pain Med. **41**(4), 501–510 (2016)
4. Abd-Elsayed, A., Kreuger, L., Wheeler, S., et al.: Radiofrequency ablation of pericranial nerves for treating headache conditions: a promising option for patients. Ochsner J. **18**(1), 59–62 (2018)
5. Lytton, W.W., Arle, J., Bobashev, G., et al.: Multiscale modeling in the clinic: diseases of the brain and nervous system. Brain Inform. **4**(4), 219–230 (2017)
6. Soloman, M., Mekhail, M.N., Mekhail, N.: Radiofrequency treatment in chronic pain. Expert Rev. Neurother. **10**(3), 469–474 (2010)
7. Calodney, A., Rosenthal, R., Gordon, A., Wright, R.E.: Targeted radiofrequency techniques. In: Racz, G., Noe, C. (eds.) Techniques of Neurolysis, pp. 33–73. Springer, Cham (2016). https://doi.org/10.1007/978-3-319-27607-6_3
8. Lundeland, B., Kvarstein, G.: Is there a place for pulsed radiofrequency in the treatment of chronic. Scand. J. Pain **12**, 55–56 (2016)
9. Makimoto, H., Metzner, A., Tilz, R.R., et al.: Higher contact force, energy setting, and impedance rise during radiofrequency ablation predicts charring: New insights from contact force-guided in vivo ablation. J. Cardiovasc. Electrophysiol. **29**(2), 227–235 (2018)
10. Zhang, B., Moser, M.A.J., Zhang, E.M., et al.: A review of radiofrequency ablation: large target tissue necrosis and mathematical modelling. Physica Med. **32**(8), 961–971 (2016)
11. Cosman Jr., E.R., Cosman Sr., E.R.: Electric and thermal field effects in tissue around radiofrequency electrodes. Pain Med. **6**(6), 405–424 (2005)
12. Sluijter, M.E., Cosman, E., Rittman, W., van Kleef, M.: The effect of pulsed radiofrequency fields applied to the dorsal root ganglion – a preliminary report. Pain Clin. **11**, 109–117 (1998)
13. Cahana, A., Zundert, J., Macrea, L., et al.: Pulsed radiofrequency: current clinical and biological literature available. Pain Med. **7**, 411–423 (2006)
14. Kroll, H.R., Kim, D., Danic, M.J., et al.: A randomized, double-blind, prospective study comparing the efficacy of continuous versus pulsed radiofrequency in the treatment of lumbar facet syndrome. J. Clin. Anesth. **20**, 534–537 (2008)

15. Snidvongs, S., Mehta, V.: Pulsed radiofrequency: a non-neurodestructive therapy in pain management. Curr. Opin. Support Palliat. Care **4**, 107–110 (2010)
16. Pangarkar, S., Miedema, M.L.: Pulsed versus conventional radio frequency ablation for lumbar facet joint dysfunction. Curr. Phys. Med. Rehabil. Rep. **4**(1), 61–65 (2014)
17. Gupta, A., Huettner, D.P., Dukewich, M.: Comparative effectiveness review of cooled versus pulsed radiofrequency ablation for the treatment of knee osteoarthritis: a systematic review. Pain Physician **20**(3), 155–171 (2017)
18. Chang, M.C.: Efficacy of pulsed radiofrequency stimulation in patients with peripheral neuropathic pain: a narrative review. Pain Physician **21**(3), E225–E234 (2018)
19. Ewertowska, E., Mercadal, B., Muñoz, V., et al.: Effect of applied voltage, duration and repetition frequency of RF pulses for pain relief on temperature spikes and electrical field: a computer modelling study. Int. J. Hyperth. **34**(1), 112–121 (2018)
20. Hasgall, P.A., Gennaro, F.D., Baumgartner, C., et al.: IT'IS database for thermal and electromagnetic parameters of biological tissues. Version 4.0, 15 May 2018. https://doi.org/10.13099/vip21000-04-0.itis.swiss/database
21. Fan, J., Wang, L.: A general bioheat model at macroscale. Int. J. Heat Mass Transf. **54**(1–3), 722–726 (2011)
22. Rohof, O.J.: Radiofrequency treatment of peripheral nerves. Pain Pract. **2**, 257–260 (2002)
23. Chua, N.H.L., Vissers, K.C., Sluijter, M.E.: Pulsed radiofrequency treatment in interventional pain management: mechanisms and potential indications - a review. Acta Neurochir. **153**(4), 763–771 (2011)
24. COMSOL Multiphysics® v. 5.2. COMSOL AB, Stockholm, Sweden. www.comsol.com
25. Topp, S.A., McClurken, M., Lipson, D., et al.: Saline-linked surface radiofrequency ablation: factors affecting steam popping and depth of injury in the pig liver. Ann. Surg. **239** (4), 518 (2004)
26. Fonseca, R.D., Monteiro, M.S., Marques, M.P., et al.: Roll off displacement in ex vivo experiments of RF ablation with refrigerated saline solution and refrigerated deionized water. IEEE Trans. Biomed. Eng. (2018). https://doi.org/10.1109/tbme.2018.2873141